Available online at www.sciencedirect.com
ScienceDirect
Geochimica et Cosmochimica Acta xxx (2010) xxx–xxx
Geochimica et Cosmochimica Acta
www.elsevier.com/locate/gca

Molecular characterization of dissolved organic matter associated with the Greenland ice sheet

Maya P. Bhatia [a], Sarah B. Das [b], Krista Longnecker [c], Matthew A. Charette [c], Elizabeth B. Kujawinski [c,*]

[a] *MIT/WHOI Joint Program in Oceanography/Applied Ocean Sciences and Engineering, Department of Geology and Geophysics, Woods Hole Oceanographic Institution, Woods Hole, MA 02543, USA*
[b] *Department of Geology and Geophysics, Woods Hole Oceanographic Institution, Woods Hole, MA 02543, USA*
[c] *Department of Marine Chemistry and Geochemistry, Woods Hole Oceanographic Institution, Woods Hole, MA 02543, USA*

Received 3 November 2009; accepted in revised form 9 March 2010

Abstract

Subsurface microbial oxidation of overridden soils and vegetation beneath glaciers and ice sheets may affect global carbon budgets on glacial–interglacial timescales. The likelihood and magnitude of this process depends on the chemical nature and reactivity of the subglacial organic carbon stores. We examined the composition of carbon pools associated with different regions of the Greenland ice sheet (subglacial, supraglacial, proglacial) in order to elucidate the type of dissolved organic matter (DOM) present in the subglacial discharge over a melt season. Electrospray ionization (ESI) Fourier transform ion cyclotron resonance (FT-ICR) mass spectrometry coupled to multivariate statistics permitted unprecedented molecular level characterization of this material and revealed that carbon pools associated with discrete glacial regions are comprised of different compound classes. Specifically, a larger proportion of protein-like compounds were observed in the supraglacial samples and in the early melt season (spring) subglacial discharge. In contrast, the late melt season (summer) subglacial discharge contained a greater fraction of lignin-like and other material presumably derived from underlying vegetation and soil. These results suggest (1) that the majority of supraglacial DOM originates from autochthonous microbial processes on the ice sheet surface, (2) that the subglacial DOM contains allochthonous carbon derived from overridden soils and vegetation as well as autochthonous carbon derived from *in situ* microbial metabolism, and (3) that the relative contribution of allochthonous and autochthonous material in subglacial discharge varies during the melt season. These conclusions are consistent with the hypothesis that, given sufficient time (e.g., overwinter storage), resident subglacial microbial communities may oxidize terrestrial material beneath the Greenland ice sheet.

1. INTRODUCTION

Anticipating how carbon flux patterns might respond to climate change is a principal motivation for understanding the different sources and reservoirs contributing to the global carbon cycle. In aquatic systems, carbon flux patterns result from complex metabolic interactions of diverse biota with a pool of organic matter (Azam, 1998). Previously it was believed that glacial environments were devoid of life and thus, that carbon dynamics in these systems should be dominated by abiotic processes (Raiswell, 1984; Chillrud et al., 1994). However, the recent discovery of large, active microbial communities beneath glaciers and ice sheets has enlightened our understanding of biogeochemical reactions and organic carbon cycling in glaciated regions, namely that subglacial microbial communities may play an active role in the carbon cycle through oxidation of organic carbon stores beneath ice masses (Sharp et al., 1999; Tranter

* Corresponding author. Address: Department of Marine Chemistry and Geochemistry, Woods Hole Oceanographic Institution, 360 Woods Hole Rd. MS#4, Woods Hole, MA 02543, USA. Tel.: +1 508 289 3493.
E-mail address: ekujawinski@whoi.edu (E.B. Kujawinski).

0016-7037/$ - see front matter © 2010 Elsevier Ltd. All rights reserved.
doi:10.1016/j.gca.2010.03.035

et al., 2002; Lanoil et al., 2009). On glacial–interglacial timescales, microbial activity might provide an important source of acidity to fuel chemical weathering of silicate rocks, a long-term control on atmospheric CO_2 levels (Berner et al., 1983; Brown, 2002). In addition, microbes may respire or ferment soil organic carbon (to CO_2 or to CH_4, respectively), previously considered inert until deglaciation (Sharp et al., 1999). Wadham et al. (2008) estimated that between 418 and 610 Pg of organic carbon was present beneath ice sheets during the last glacial period, of which 63 Pg C was available for conversion to methane over a glacial cycle. Additionally, Skidmore et al. (2000) calculated that aerobic respiration of subglacial organic carbon could convert 8.1 Pg C to carbon dioxide over a glacial cycle. These calculations, however, are constrained by a lack of knowledge concerning the availability of the subglacial organic carbon stores to microbial degradation. This is a potentially large limitation, given the range in biological reactivity within all other organic carbon stores (Hedges et al., 2000; Eglinton and Repeta, 2003). In order to examine the impact of microbial oxidation on subglacial organic carbon stores, it is critical to assess the composition and reactivity of this material.

Carbon is derived from two distinct regions of the glacial environment: (1) on the glacier surface (i.e., the supraglacial environment) from inorganic and organic carbon in snow and ice; and (2) at the glacier base (i.e., the subglacial environment) where carbon is derived from the underlying bedrock, sediments, and ice. These two regions are linked by a hydrological network that becomes activated during the summer melt season when accumulated surface meltwaters drain through crevasses, moulins, and englacial channels to the bed (e.g. Nienow et al., 1998; Das et al., 2008). Once at the bed, the supraglacial meltwaters become connected to a broad subglacial hydrological drainage network, in contact with the underlying till and bedrock (Nienow et al., 1998). Generally, dissolved organic carbon (DOC) concentrations in supraglacial snow and meltwater are very low (~10–40 μM) (Lafreniere and Sharp, 2004; Lyons et al., 2007). In contrast, available organic carbon sources in subglacial environments have variable DOC concentrations ranging from 60 to 700 μM as reflected in subglacial outflow waters (Lafreniere and Sharp, 2004; Skidmore et al., 2005) and concentrations up to ~4 mM (Dry Valleys, Antarctica) and ~20 mM (Ellesmere Island, Canada) in basal ice samples (Barker et al., 2006; Bhatia et al., 2006). Although measurements are limited, this variability observed among subglacial DOC concentrations is likely a function of sampling time and/or of different physical characteristics (e.g. lithologies, sediment content, proximity to land) between and within specific field sites.

While bulk DOC abundance studies are useful as first-order investigations, they offer little information regarding the provenance, reactivity and bioavailability of the glacial organic carbon pools. In an effort to address these issues, Lafreniere and Sharp (2004) and Barker et al. (2006) used spectrofluorometric techniques to distinguish subglacial fulvic acids (the portion of humic material which is water-soluble at any pH) derived from terrestrial precursor material from those of microbial origin. Terrestrially derived dissolved organic matter (DOM) would contain fulvic acids from plant and soil organic matter, which are typically more aromatic, due to the presence of compounds such as lignins (McKnight et al., 2001). Alternatively, microbially-derived DOM would contain fulvic acids from microbial cell components and metabolism, and are typically less aromatic (McKnight et al., 1994; McKnight et al., 2001). Both Lafreniere and Sharp (2004) and Barker et al. (2006) found that supraglacial samples contained microbially-derived fulvic acids, which they attributed to primary productivity of algae and bacteria in the snow, ice, and meltwater on the glacial surface. However, results from the subglacial runoff were more variable, with both studies finding sources of fulvic acids with both microbial and terrestrial provenance. These findings were attributed to changing subglacial flow-routing regimes throughout the melt season that access different carbon pools as well as to *in situ* subglacial microbial metabolisms that alter the subglacial carbon pools.

Though an important first step in compositional assessment of glacial organic carbon pools, fluorescence spectroscopy studies are limited because (1) they can only assess one fraction of DOM (fulvic acids), and (2) they do not directly identify the presence of specific compounds within the DOM pool, thus permitting only broad distinctions between 'microbial' and 'terrestrial' components. In contrast, electrospray ionization (ESI) coupled to Fourier transform ion cyclotron resonance mass spectrometers (FT-ICR MS) provides an opportunity to study a larger portion of the DOC pool (intact polar molecules), and to characterize the reactivity of specific molecules in biogeochemical processes. ESI is a 'soft' (low-fragmentation) ionization technique that detects polar molecules with acidic and basic functional groups. When coupled to a mass spectrometer, such as FT-ICR MS which is capable of ultrahigh mass resolution (>100,000) and mass accuracy (<1 ppm), tens of molecules can be accurately resolved at each nominal mass (Kujawinski, 2002; Marshall and Rodgers, 2008). The mass accuracy achievable is the key to this technique as it enables the assignment of elemental formulae solely from the mass measurement (Kim et al., 2006; Kujawinski and Behn, 2006). Therefore, ESI FT-ICR MS can be used to identify compositional differences among pools of DOM, as well as to determine the elemental compositions of specific molecules within DOM. Recently, ESI FT-ICR MS has been utilized to characterize DOM in a range of diverse environments, including freshwater systems (Sleighter and Hatcher, 2008), marine systems (Koch et al., 2005), and ice cores (Grannas et al., 2006).

The goal of this study was to investigate the compositional nature of carbon pools associated with different regions of the Greenland ice sheet in order to elucidate the type of dissolved organic matter present in the subglacial discharge over a melt season. The carbon pools explored were (1) the supraglacial environment: snow and meltwater on the ice surface, (2) the subglacial environment: water exiting the base of a land-terminating outlet glacier, and (3) the proglacial tundra environment: non-glacially derived pond water. From a hydrological perspective, these environments are serially connected to each other as the

Please cite this article in press as: Bhatia M. P., et al. Molecular characterization of dissolved organic matter associated with the Greenland ice sheet. *Geochim. Cosmochim. Acta* (2010), doi:10.1016/j.gca.2010.03.035

majority of the supraglacial meltwater on a glacier surface penetrates to the subglacial environment and eventually exits into the proglacial environment. Thus, the compositional characteristics of the contributing carbon pools as well as physical and microbial processes en route ultimately dictate the composition of the DOM in the subglacial discharge. We employed ESI FT-ICR MS to detect compositional differences among the different carbon pools sampled, and to gain insight into the molecular-level impact of microbial metabolism on subglacial organic carbon. By establishing baseline values of the type of organic carbon present beneath glaciated areas, this study serves as the foundation for broader investigations into the impact of increased meltwater runoff from the Greenland ice sheet to surrounding marine environments, and into the extent of subglacial microbial oxidation of overridden soils and vegetation.

2. METHODS

2.1. Field sites

This study was conducted at two locations along the western margin of the Greenland ice sheet in 2007 and 2008. In July 2007 two snow samples and one supraglacial meltwater sample were collected from the ablation zone on the ice sheet surface, at 980-m elevation approximately 40 km inland from the edge of the ice sheet (Fig. 1). By July most of the seasonal snow deposited the previous winter had already melted, thus our samples were collected from isolated pockets of heavily metamorphosed and colored snow from drifts along the banks of relict stream channels. Of the two snow samples analyzed for this study, one exhibited a yellow and green hue (Yellow Snow) and the other a red and black hue (Red Snow). The supraglacial meltwater sample (Supraglacial Inland) was collected from the edge of a large meltwater lake (~1 km in diameter). Given the scarcity of seasonal snow on the ice sheet surface during our sampling period, and the high annual ablation rates we measured at this site (~2-m ice melt yr^{-1}), this meltwater sample is assumed to be derived almost entirely from glacial ice melt rather than from seasonal snow melt or rainfall.

In May and July 2008, samples were collected in the vicinity of a small land-terminating outlet glacier (named glacier 'N' here), approximately 70 km south of the 2007 site (Fig. 1). In May, one sample was collected from a small supraglacial meltwater pond (~20 m in diameter) within 1 km of the ice sheet margin (Supraglacial Margin). The water here consisted primarily of snow and ice melt. A second sample was collected from the subglacial stream exiting at the base of glacier 'N' (Subglacial May). A third sample was collected at a proglacial pond (Tarn). In July, two additional samples were collected from the subglacial stream exiting the base of glacier 'N' (Subglacial July-1 and Subglacial July-2, referred to collectively as Subglacial July). A synopsis of the samples collected in this study and the filtration and extraction procedures (details below) is presented in Table 1. Electrical conductivity (EC) measurements were made on-site using a Russell RL060C meter (Thermo Electron) for the Subglacial May and July and Supraglacial Margin samples, and are also presented in Table 1.

2.2. Sample collection and filtration

The snow samples were collected aseptically using sterile plastic bags (WhirlPak; Nasco Products), and melted onsite in a warm water bath; conditions in the field precluded melting the samples at a controlled 4 °C. The water samples were collected in either combusted glass or acid-cleaned Teflon bottles. All samples were filtered on-site through 0.2-μm filters prior to extraction, except for the Red Snow sample, which was processed back in the laboratory. Most samples (Yellow Snow, Supraglacial Inland, Supraglacial Margin, Subglacial May, Tarn) were filtered using 0.2-μm Sterivex cartridges (Millipore), that had been pre-cleaned by soaking in a 10% HCl bath for at least one day, followed by rinsing with 20 L of Milli-Q water. The background DOC concentration of the pre-cleaned units was approximately 9 μM. Due to limited availability of pre-cleaned Sterivex units in the field, the remaining samples (Red Snow, Subglacial July-1, Subglacial July-2) were filtered through a combusted GFF (Whatman) pre-filter and a combusted 0.2-μm Anodisc membrane (Whatman). All solvents were purchased from Thermo Fisher Scientific (Waltham, MA) and were Optima grade or better. Concentrated HCl was Trace-Metal grade. The final volumes of 0.2-μm filtrate (Table 1) differed to accommodate a range of anticipated DOC contents as well as the difficulties encountered with filtering some samples (for example, Subglacial May contained a significant amount of rock flour that quickly clogged the filters). An aliquot of the 0.2-μm filtrate was acidified and stored in a combusted vial for DOC analysis.

2.3. Solvent extraction

Immediately following 0.2-μm filtration, all samples were acidified to pH 3 with 12 M HCl and dissolved organic matter (DOM) was extracted with either C_{18} cartridges (Mega Bond Elut, UTC) or C_{18} extraction discs (3 M) (Table 1). All of the solvent extractions except for the Subglacial July and Red Snow samples were done on-site. The Subglacial July and Red Snow samples were kept as cold as possible, and extracted approximately two months later. The solvent extraction protocol employed was modified from Kim et al. (2003b). Briefly, the cartridges or discs were pre-cleaned according to manufacturer's instructions. The acidified sample was then passed through the cleaned cartridge/disc and the cartridge/disc was left to dry for 15 min prior to solvent extraction with methanol (MeOH) (Table 1). Extracts were evaporated to dryness under vacuum at 30 °C. For Red Snow, the 70% and 100% MeOH aliquots were combined prior to vacuum evaporation. A procedural blank (MeOH) was also evaporated to dryness under vacuum. The samples and solvent blank were stored dry at −20 °C until further analysis. We estimated our DOM extraction efficiency by drying an aliquot of the solvent extract on a pre-weighed combusted GFF, and measuring the carbon by dynamic flash combustion on a ThermoQuest EA1112 Carbon/Nitrogen Analyzer. The

Please cite this article in press as: Bhatia M. P., et al. Molecular characterization of dissolved organic matter associated with the Greenland ice sheet. *Geochim. Cosmochim. Acta* (2010), doi:10.1016/j.gca.2010.03.035

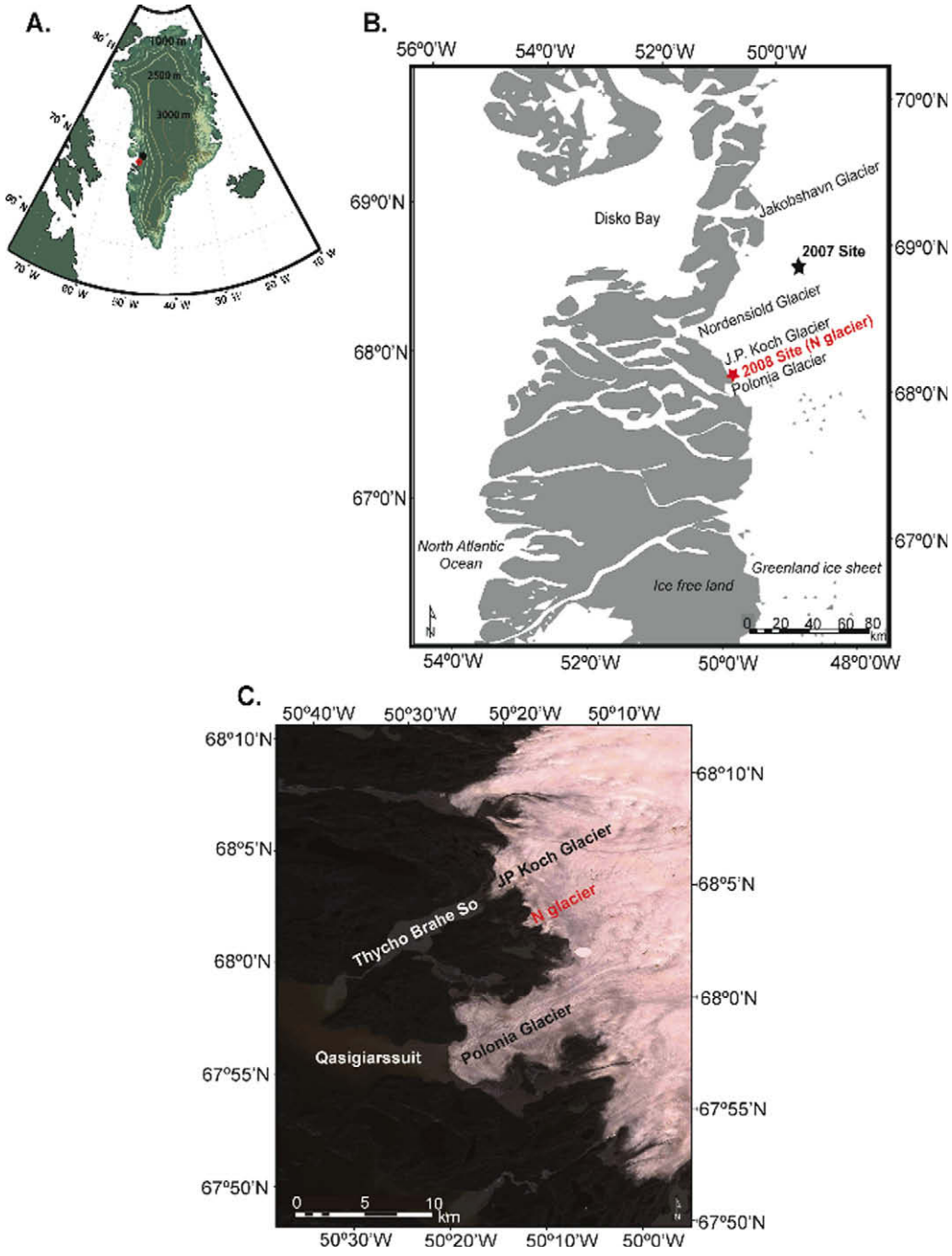

Fig. 1. Locations of the 2007 and 2008 sample sites. (A) A map of Greenland, with the black circle representing the 2007 field site and the red circle representing the 2008 field site. The green contour lines represent the surface elevation (5-km DEM from Bamber et al., 2001; Layberry and Bamber, 2001). (B) An expanded image of the two field sites. The 2007 ice surface field site is ~40 km inland from the ice sheet edge, and approximately 70 km north of the 2008 field site, located at the glacier margin. (C) A Landsat image of the 2008 ice marginal sample location (named 'N' glacier in this study). (For interpretation of the references to colour in this figure legend, the reader is referred to the web version of this article.)

extraction efficiency for each sample was calculated as the percent of carbon recovered from the solvent extract relative to the total amount of carbon in the sample (as determined by TOC analysis). The extraction efficiencies (Table 1) ranged from 10% to 94%, with a mean of 44% and a median of 28%. Although we obtained a low extraction efficiency (10%) for the Subglacial July-2 sample, we do not anticipate being limited in our conclusions since this sample is duplicated by Subglacial July-1 and the mass spectral characteristics of the two samples are nearly identical (see Section 3.2 and Fig. 3). The Tarn sample was the one most similar to previously described freshwater

Please cite this article in press as: Bhatia M. P., et al. Molecular characterization of dissolved organic matter associated with the Greenland ice sheet. *Geochim. Cosmochim. Acta* (2010), doi:10.1016/j.gca.2010.03.035

Table 1
Synopsis of the samples collected in this study in preparation for DOM extraction and mass spectrometry analysis. (*) – The [DOC] reported for Subglacial July-1 is from a sample collected 6 h prior to the sample analyzed for DOM composition in this study. N/A = data not available.

Region	Sample	Collection date	Location	Volume filtered	C_{18} DOM extraction	Solvent extract	DOC concentration(μM)	Electrical conductivity (μS/cm^3)	Extraction efficiencies (%)
Snow	Yellow Snow	July 17 2007	68°33′N49°23′W	2 L	Cartridge	40 mL 100% MeOH	N/A	N/A	N/A
Snow	Red Snow	July 17 2007	68°34′N49°22′W	87 mL	Discs	5 mL 70%, 5 mL 100% MeOH	N/A	N/A	N/A
Supraglacial	Supraglacial Inland	July 14 2007	68°34′N49°21′W	15 L	Cartridge	40 mL 100% MeOH	N/A	N/A	N/A
Supraglacial	Supraglacial Margin	May 31 2008	68°02′N50°15′W	4 L	Cartridge	15 mL 100% MeOH	16 ± 0.7	0.2	28
Subglacial	Subglacial May	May 31 2008	68°02′N50°16′W	500 mL	Cartridge	15 mL 100% MeOH	28 ± 0.2	17	94
Proglacial	Tarn	May 292008	68°02′N50°17′W	1 L	Cartridge	15 mL 100% MeOH	406 ± 3	N/A	57
Subglacial	Subglacial July-1	July 122008	68°02′N50°16′W	4.5 L	Cartridge	15 mL 100% MeOH	*15 ± 0.4	3.2	28
Subglacial	Subglacial July-2	July 162008	68°02′N50°16′W	3.45 L	Cartridge	15 mL 100% MeOH	51 ± 0.3	2.3	10

samples and the extraction efficiency of this sample (60%) is well within the range documented to other freshwater studies (Kim et al., 2003b; Dittmar et al., 2008).

2.4. DOC concentrations

Total and dissolved organic carbon (TOC, DOC) concentrations were quantified as non-purgeable organic carbon (NPOC) by high temperature combustion (680 °C) with a Shimadzu TOC-V_{CSH} analyzer equipped with a high sensitivity platinum catalyst (Shimadzu Scientific Instruments). Samples were quantified using a 5-point standard curve made with potassium hydrogen phthalate (KHP). Blanks and reference standards were analyzed routinely within each sample run. Reference standards for low carbon water and deep-sea water were obtained from the Consensus Reference Materials Project, Hansell Laboratory, University of Miami. DOC was not quantified for the 2007 samples due to post-acquisition contamination in Greenland.

2.5. FT-MS data acquisition

All samples and the solvent blank were analyzed on a 7-T ESI FT-ICR mass spectrometer (LTQ-FT-MS, Thermo Fisher Scientific, Waltham, MA). For positive ion mode analyses, sample aliquots were reconstituted in 80% MeOH with 0.1% acetic acid (final concentration). Acetic acid promoted positive ion formation. For negative ion mode analyses, reconstituted sample aliquots were reconstituted in 70% MeOH. The solvents used to dilute the samples were also analyzed as instrument blanks (100% MeOH in positive ion mode and 70% MeOH in negative ion mode).

For both positive and negative ion modes, samples were infused into the ESI interface at 4 μL min^{-1}, and instrument parameters were optimized for each sample. Samples were diluted to optimize spray conditions; dilutions ranged from 1:5 to 1:40. The capillary temperature was set at 250 °C, and the spray voltage varied between 4.40 and 4.60 kV. About 200 scans were collected for each sample, a sufficient number of scans for peak reproducibility in our samples. The mass ranges for full-scan collection were $200 < m/z < 1200$ and $200 < m/z < 1000$ in positive and negative ion modes, respectively. Weekly mass calibrations were performed with an external standard (Thermo Calibration Mix), and resulted in mass accuracy errors <1 ppm. The target average resolving power was 400,000 at m/z 400 (where resolving power is defined as $m/\Delta m_{50\%}$ where $\Delta m_{50\%}$ is the width at half-height of peak m). Good quality data could not be collected for the Subglacial July-2 sample in positive ion mode, nor for the Red Snow sample in negative ion mode. This was due to unacceptable spray stabilities in the former and fluctuating ion currents in the latter.

Please cite this article in press as: Bhatia M. P., et al. Molecular characterization of dissolved organic matter associated with the Greenland ice sheet. *Geochim. Cosmochim. Acta* (2010), doi:10.1016/j.gca.2010.03.035

2.6. FT-MS data analysis

2.6.1. Peak detection and blank correction

We collected individual transients as well as a combined raw file using *xCalibur 2.0*. Transients were co-added and processed with custom-written MATLAB code provided by Southam et al. (2007). This code was used as provided with the following parameters. Within each sample, only those transients whose total ion current (TIC) was greater than 20% of the maximal TIC were co-added and then processed with Hanning apodisation, and zero-filled once prior to fast Fourier transformation. We retained all *m/z* values with a signal-to-noise ratio above 5 (as calculated in Southam et al. (2007)). The individual sample and solvent blank peak lists were then aligned using MATLAB code provided by Mantini et al. (2007). Positive and negative ion mode data were aligned separately in MATLAB with an error tolerance of 1 ppm. Following alignment, all peaks found in each mode's solvent blanks were removed from the appropriate master list. These blank-corrected master peak lists in each sample were used in all downstream statistical analyses and elemental formula assignments.

2.6.2. Calibration

Positive and negative ion mode spectra were internally re-calibrated using a short list of *m/z* values present in a majority of samples. This list of calibrants was chosen according to the following criteria: (1) presence in the majority of samples; (2) elemental formulae could be assigned with C, H, O and N; (3) similar mass errors for all; and (4) distribution along the *m/z* range of each spectrum. The resulting calibrants and their elemental formulae are provided in EA Table 1a and b. After internal re-calibration, the root mean square (RMS) errors for the calibrants ranged from 0.09 to 0.12 in positive ion mode and 0.04 to 0.69 in negative ion mode.

2.6.3. Elemental formula assignments

Elemental formulae were assigned to the aligned blank-corrected peaks (*m/z* values) using the Compound Identification Algorithm (CIA), described by Kujawinski and Behn (2006) and modified in Kujawinski et al. (2009). In the CIA, we set the following parameters: (a) formula error was 1 ppm, (b) the relationship error was 20 ppm, and (c) the mass limit above which elemental formulae were only assigned by functional group relationships was 500 Da. For this study, elemental formulae were determined for *m/z* values below 500 Da by comparison to an in-house database of mathematically and chemically legitimate formulae within the 1 ppm error window. Elemental formula assignments were constrained to ^{12}C, ^{13}C, ^{1}H, ^{16}O, ^{14}N, ^{34}S, and ^{31}P. Error testing for formula assignments containing these elements was done using synthetic datasets and is documented in Kujawinski and Behn (2006). Accuracy of formula assignments ranges from 78% to 100%, depending on included elements (Kujawinski and Behn, 2006). These elemental formulae were extended to *m/z* values above 500 Da through identification of functional group relationships. The functional group relationships used by CIA are common to refractory dissolved organic matter (e.g. humic acids); CIA does not presently include many functional group relationships resulting from metabolic (biological) reactions (Kujawinski and Behn, 2006). Isotopomers with a ^{13}C atom are identified in the last step of CIA and elemental formulae are corrected to reflect ^{13}C content. In order to identify terrestrially-derived components of our samples, we compared the elemental formulae for our Greenland samples with those assigned to Suwannee River Fulvic Acid Standard I (Suwannee River – International Humic Substances Society, Stock #1S101F), previously analyzed in our laboratory with negative ion mode ESI FT-ICR MS. Magnitude-averaged elemental ratios and double bond equivalencies were calculated (Sleighter and Hatcher, 2008).

2.6.4. Assessment of potential contamination

Analysis of the negative and positive ion mode mass spectra revealed potential contamination likely originating from plasticizers or the C_{18} extraction cartridges/discs. In negative ion mode, potential contamination was most prevalent in the Yellow Snow sample. We assigned elemental formulae to the contaminated *m/z* values (18 peaks) and identified peaks belonging to this series in other negative ion mode spectra. Contaminated peaks did not occupy any particular region of the van Krevelen diagram (EA Fig. 1). We realize that any contamination may skew the overall composition of the DOM through ion suppression; nonetheless, we believe we attained an adequate representation of DOM composition within our samples because the maximum percentage of peaks represented by the suspected plasticizer contamination was less than 0.6% in any one sample. In addition, to further minimize the potential impact of this contamination, we based our statistical analyses and subsequent conclusions on the diversity of resolved peaks (presence/absence) rather than on their relative peak heights. In positive ion mode, the potential contamination was more pervasive. Inspection of the raw mass spectra revealed likely contamination in the Yellow Snow, Subglacial May, and Tarn samples. Given this observation, we focused our statistical analyses and interpretations on the negative ion mode dataset.

2.6.5. Multivariate statistics

We assessed differences in our samples in negative ion mode with cluster analysis as described in Kujawinski et al. (2009). In our analysis, we transformed all relative peak heights to presence (peak height = 1) or absence (peak height = 0). We recognize that ESI is not quantitative and that differences in ionization efficiencies among compounds can lead to misrepresentations of ion peak height, relative to the abundance of the parent molecule in neutral solution (Stenson et al., 2003). To circumvent this known problem, we have used presence/absence comparisons rather than those that rely on relative peak height.

The presence/absence transformation allows assessment of how samples differ based solely on peak diversity. A distance matrix was calculated between all the samples in each mode using the Bray–Curtis distance measure (MATLAB code written by David Jones, University of Miami, as part of the Fathom toolbox); a distance measure of 0 indicates samples are identical with regards to peak diversity,

Please cite this article in press as: Bhatia M. P., et al. Molecular characterization of dissolved organic matter associated with the Greenland ice sheet. *Geochim. Cosmochim. Acta* (2010), doi:10.1016/j.gca.2010.03.035

whereas a distance measure of 1 indicates that samples share none of their peaks. Ward's linkage method was used to group the samples followed by presentation of the results as a dendrogram.

2.6.6. Indicator species analysis

We identified specific *m/z* values characteristic of the observed negative ion mode cluster groupings with indicator species analysis (ISA – as implemented in Kujawinski et al., 2009). ISA combines the relative abundance and relative frequency of a peak within a pre-defined group of samples to assign an indicator value (IV) to each peak (McCune and Grace, 2002). A perfect IV (equal to 100) of a particular group would constitute an *m/z* value that was present exclusively in the samples comprising that group (McCune and Grace, 2002). Statistical significance of IVs is calculated by comparison with Monte-Carlo simulations of randomized data. ISA requires a priori assignment of samples to groups; this was achieved using the protocol and criteria described in McCune and Grace (2002). The best number of groups occurred when we used four groups of samples: Group 1 = Yellow Snow; Group 2 = Supraglacial Inland; Group 3 = 'N' glacier May samples (Subglacial May and Supraglacial Margin); and Group 4 = 'N' glacier July and Tarn samples (Subglacial July-1, 2 and Tarn). This group assignment was used to find indicator *m/z* values for Groups 3 and 4; use of ISA is restricted to those groups with more than one sample, thus no 'indicator peaks' were identified for Groups 1 and 2. The final list of indicator *m/z* values for each group was manually curated using the criteria outlined in Kujawinski et al. (2009).

3. RESULTS AND DISCUSSION

3.1. Sample overview

The eight samples analyzed in this study represent carbon pools associated with different regions of a glacier system. The supraglacial pools are represented by snow (Yellow Snow, Red Snow) and meltwater (Supraglacial Inland) samples from the inland ice surface as well as the meltwater sample collected on the surface of 'N' glacier (Supraglacial Margin). The subglacial pool at the glacier base is represented by samples collected from the subglacial stream exiting at the base of 'N' glacier (Subglacial May, Subglacial July-1, 2). Since surface ice melting is minimal in May, the Subglacial May water sample most likely represents early/spring discharge waters that have been stored at the bed overwinter. These waters likely drain a more distributed subglacial hydrological system with relatively slower flow rates, but they may access a greater areal extent of the subglacial bed (Nienow et al., 1998; Sharp et al., 1999). Conversely, the July subglacial water samples represent late/summer discharge waters fed primarily by supraglacial inflow. These waters likely drain through a channelized hydrological system characterized by relatively much higher flow rates, but they may access a more limited part of the bed (Bingham et al., 2005; Nienow et al., 1998). The electrical conductivity (EC) measurements (Table 1) support this interpretation. The Subglacial May sample has a greater content of dissolved solutes compared to the Subglacial July samples. Finally, a proglacial tarn (Tarn) represents a terrestrial carbon end-member, comprised of non-glacial water, situated in the deglaciated arctic tundra and likely containing a large terrestrial contribution from the surrounding vegetation.

3.2. Comparison of ultra-high resolution mass spectra

All of the samples contained highly complex DOM with numerous peaks per nominal mass in both positive and negative ion modes. The total numbers of peaks resolved in each sample in negative ion mode following blank correction are presented in Table 2. Qualitative differences among the raw mass spectra illustrate that samples representing different regions of the Greenland ice sheet have distinct

Table 2
Synopsis of general parameters regarding negative ion mode formula assignments. Elemental ratios were calculated as magnitude-averaged values (Sleighter and Hatcher, 2008) for *m/z* values with assigned elemental formulae.

Sample	Total number of peaks	Number of formulas assigned	% Formulas assigned	$H:C_w$	$O:C_w$	$N:C_w$	$S:C_w$	$P:C_w$	DBE_w	% Formulae with CHO	% Formulae with CHON	% Formulae with CHONP, CHONS, CHONSP
Yellow Snow	5113	4380	85.7	1.22	0.41	0.30	0.04	0.05	9.79	17.4	23.4	42.5
Supraglacial Inland	1865	1169	62.7	1.16	0.40	0.33	0.03	0.05	12.15	1.7	32.0	50.1
Supraglacial Margin	2331	1980	84.9	1.68	0.27	0.27	0.01	0.03	6.21	23.3	34.7	25.0
Subglacial May	1737	1662	95.7	1.56	0.38	0.17	0.00	0.01	6.66	55.6	26.1	11.3
Subglacial July-1	3330	3249	97.6	1.26	0.38	0.16	0.00	0.02	9.62	69.2	8.1	18.9
Subglacial July-2	3048	2800	91.9	1.24	0.38	0.21	0.00	0.02	10.08	58.9	10.8	26.2
Tarn	5958	5826	97.8	1.27	0.43	0.12	0.00	0.01	10.28	65.7	12.3	17.5
Suwannee River	2092	2079	99.4	1.05	0.55	0.03	0.00	0.01	10.85	91.3	2.0	4.5

Please cite this article in press as: Bhatia M. P., et al. Molecular characterization of dissolved organic matter associated with the Greenland ice sheet. *Geochim. Cosmochim. Acta* (2010), doi:10.1016/j.gca.2010.03.035

DOM compositions (Fig. 2). Although ultra-high resolution mass spectrometry has not been used to date to compare DOM from different glacial sub-environments, this result is not surprising since both bulk DOC concentrations and *in situ* microbial communities can differ vastly among glacial sub-environments (Bhatia et al., 2006).

Cluster analysis based on the presence/absence of resolved peaks in negative ion mode (Fig. 3) revealed that the samples collected on the inland ice sheet (Yellow Snow, Supraglacial Inland) were distinct from each other as well as from those collected at the ice sheet margin (Subglacial May, Supraglacial Margin, Tarn, Subglacial July-1, 2). Indeed, the Yellow Snow and Supraglacial Inland samples share very few peaks (<20%) with any of the samples collected at the ice margin (Table 3). The cluster analysis for positive ion mode data (not shown) confirmed that the three samples from the inland ice sheet surface (Yellow Snow, Red Snow, and Supraglacial Inland) were distinct from the ice margin samples (Subglacial May, Supraglacial Margin, Tarn, Subglacial July-1). Differentiation between these sample groups is expected since the Yellow Snow and Red Snow should represent very different, localized regions on the ice sheet surface with unique algal and microbial communities. The lack of similarity between the supraglacial meltwater samples (Supraglacial Inland and Supraglacial Margin, only sharing 13% and 10% of their peaks respectively, Table 3) could be attributed to geographical, seasonal and water source differences. For

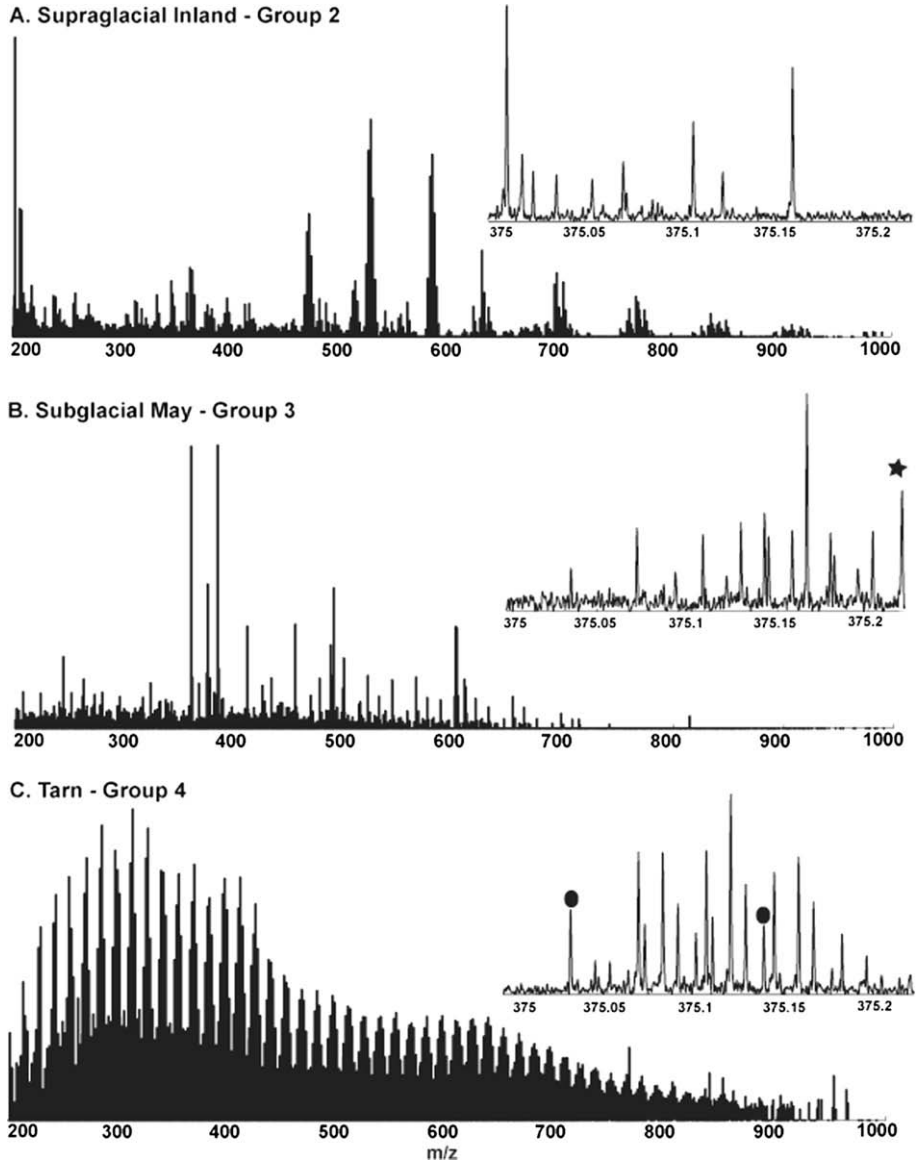

Fig. 2. Negative ion mode blank-corrected, calibrated mass spectra from the groups identified in indicator species and cluster analysis. Group 1: Yellow Snow (not shown); Group 2: Supraglacial Inland; Group 3: N glacier May (Subglacial May and Supraglacial Margin); and Group 4: terrestrial/N glacier July (Tarn and Subglacial July-1, 2). The inset shows the region $375.0 \leqslant m/z \leqslant 375.2$ and the indicator m/z values for Group 3 (black stars) and Group 4 (black ovals).

Please cite this article in press as: Bhatia M. P., et al. Molecular characterization of dissolved organic matter associated with the Greenland ice sheet. *Geochim. Cosmochim. Acta* (2010), doi:10.1016/j.gca.2010.03.035

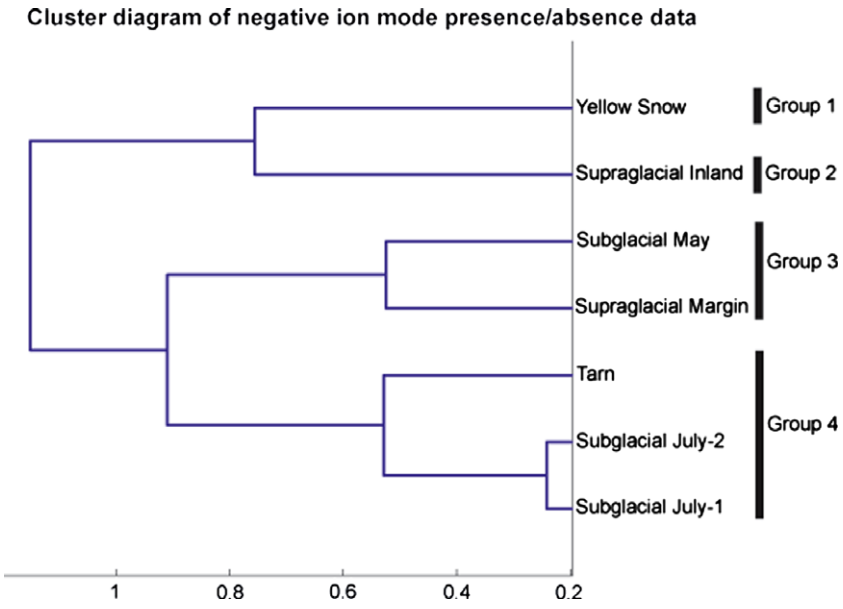

Fig. 3. Cluster diagram of the seven negative ion mode samples, based on Bray–Curtis distance measure and Ward's linkage method.

Table 3
Percentage of negative ion mode peaks shared between the different samples analyzed in this study and Suwannee River.

Sample	Yellow Snow	Supraglacial Inland	Supraglacial Margin	Subglacial May	Subglacial July-1	Subglacial July-2	Tarn	Suwannee River
% Yellow Snow shared with	100	17	16	13	15	15	18	9
% Supraglacial Inland shared with	46	100	13	7	11	14	9	4
% Supraglacial Margin shared with	35	11	100	42	39	35	35	11
% Subglacial May shared with	39	7	56	100	61	56	60	36
% Subglacial July-1 shared with	23	6	27	32	100	73	79	39
% Subglacial July-2 shared with	24	9	27	32	79	100	73	39
% Tarn shared with	16	3	14	18	44	37	100	25
% Suwannee River shared with	22	4	12	29	62	57	70	100

example, the Supraglacial Inland sample was collected from a large supraglacial lake composed almost entirely of inland ice melt. In contrast, the Supraglacial Margin sample was collected from a small meltwater pool closer to the ice edge and much earlier in the melt season, and thus is comprised of a mixture of marginal snow and ice melt.

Among the margin-site samples, results from the cluster analyses for positive and negative ion modes indicate that the DOM composition in the subglacial runoff changes during the melt season. Specifically, the negative ion mode cluster analysis illustrates that the 'N' glacier May samples (Supraglacial Margin and Subglacial May) were grouped (sharing 42% and 56% of their peaks respectively, Table 3) as were the Subglacial July-1, 2 and Tarn samples (Subglacial July samples sharing 73–79% of their peaks with the Tarn sample, Table 3). Interestingly, the Subglacial July samples are quite distinct from the Subglacial May sample even though the two samples were collected from the same location. In addition, there is significant peak overlap between Suwannee River and the Tarn sample (70%) and between the Subglacial July samples (57–62%), but much less between Suwannee River and the Subglacial May sample (30%). Thus, although our samples are temporally limited (May and July), we infer that the type of DOM in subglacial discharge changed during the 2008 melt season.

3.3. Elemental formula assignments and indicator species analysis

We were able to assign formulae to over 90% of the resolved peaks in the Suwannee River and the Tarn, Subglacial July-1, 2, and Subglacial May samples. We achieved slightly lower percentages of formulae assigned to the Yellow Snow (86%) and Supraglacial Margin (85%) samples, with the

Please cite this article in press as: Bhatia M. P., et al. Molecular characterization of dissolved organic matter associated with the Greenland ice sheet. *Geochim. Cosmochim. Acta* (2010), doi:10.1016/j.gca.2010.03.035

lowest percentage of formulae found for the Supraglacial Inland sample (63%). In an effort to increase the percentage of formula assignments in this sample, we made two temporary modifications to CIA. First, we included halogens (F, Cl, Br, and I) in our formula assignments; and second, we attempted to account for multiply-charged molecules. Inclusion of halogens did not increase our formula assignment rate appreciably. In contrast, corrections for doubly- and triply-charged molecules produced a marked increase in the Supraglacial Inland formula assignment percentage (up to 98%), suggesting that a good portion of our *m/z* values represented multiply-charged molecules with multiple de-protonation sites. We discarded these improvements, however, because the modified CIA lowered the formula assignment accuracy when tested with Suwannee River formulae and because multiply-charged isotopomers were rarely available for reliable charge-state determination. Thus, we were forced to retain the original lower formula assignment percentages made to the Supraglacial Inland sample.

Elemental formulae containing only C, H, and O dominated the formula assignments for the Tarn and subglacial samples (Subglacial May and Subglacial July-1, 2) (Table 2). Conversely, the supraglacial samples were dominated by formulae containing C, H, O, and N (Supraglacial Margin), or C, H, O, N, and S/P (Yellow Snow, Supraglacial Inland) (Table 2). We should note that this result differs from analysis of other supraglacial organic material in ice cores collected from Russia where formulae containing C, H, and O were the most abundant (Grannas et al., 2006). However, the snow and meltwater samples analyzed in this study (i.e., collected from marginal areas where there is snow melt and water in the residual snowpack) are quite different from bulk ice core material (i.e., collected from inland areas where ice is formed in the dry snow zone), so it is not surprising that we resolved different compounds.

For comparison with other DOM compositional studies, we calculated the magnitude-averaged bulk elemental ratios and double-bond equivalency (DBE) for all samples (Table 2) (Koch et al., 2008; Sleighter and Hatcher, 2008). Molecular H:C and O:C ratios have been reported previously to range broadly from 0.3 to 1.8 and 0 to 0.8, respectively (Koch et al., 2008; Sleighter and Hatcher, 2008; Stenson et al., 2003). The elemental ratios of all of our samples fall within this range (Table 2), with Suwannee River being the most aromatic (H:C = 1.05), and the Subglacial May and Supraglacial Margin samples being the most aliphatic (H:C = 1.68 and 1.56, respectively). The low DBE of the Supraglacial Margin and Subglacial May samples also imply that DOM in these samples is relatively aliphatic. The DBE was the highest in the Supraglacial Inland sample. This fact, combined with the relatively lower H:C ratio (1.16) and relatively higher N:C ratio (0.33) of this sample (Table 2), suggest that molecules within this sample may contain condensed nitrogen functionalities (i.e., aromatic nitrogen or nitro groups). Finally, the supraglacial samples (Yellow Snow, Supraglacial Inland, Supraglacial Margin) generally had relatively high N:C ratios (0.30, 0.33, 0.27, respectively, Table 2), suggesting that nitrogen-containing molecules could be major contributors to DOM in these samples (Reemtsma et al., 2008).

Van Krevelen diagrams were generated for all Greenland samples and Suwannee River in order to compare DOM composition across our samples (representative sample plots in Fig. 4). Van Krevelen diagrams illustrate the O:C molar ratio and the H:C molar ratio of each elemental formula on the *x*- and *y*-axes, respectively. Generally, major biogeochemical compound classes (such as condensed hydrocarbons, lipids, proteins, lignins, and carbohydrates) have characteristic H:C and/or O:C molar ratios, and thus should occupy specific regions of the plot (Kim et al., 2003a; Wu et al., 2004; Kujawinski and Behn, 2006). The percentages of negative ion mode formula assignments located in the different regions of the van Krevelen diagram are presented in Table 4. However, we should note that van Krevelen diagrams should be interpreted with caution as inconsistent definitions of particular compound classes across the literature (e.g., lipid), and variable O:C or H:C ratios within particular compound classes (e.g., proteins) may lead to exclusion of elemental formulae from the prescribed compound class regions (Kujawinski and Behn, 2006). Nonetheless, at present, they remain the best way to graphically depict elemental formula assignments for mass spectra comprised of thousands of peaks.

The van Krevelen plot of the negative ion mode Suwannee River sample (not shown) is consistent with previous work (Stenson et al., 2003). Over 99% of formulae were assigned and most occur in the region associated with lignin-derived materials (Stenson et al., 2003). Very few formulae are present in the regions associated with proteins and lipids (Table 4). Because of these results and the fact that Suwannee River is well-cited as a terrestrial DOM endmember (e.g. McKnight et al., 2001; Stenson et al., 2003), we label the region encompassing the majority of its elemental formula assignments as "terrestrial" (shown in Figs. 4 and 5), and use this information to aid our analyses of our negative ion mode spectra.

The van Krevelen diagrams may explain the observed cluster groupings in Fig. 3. In negative ion mode, the separation between the samples collected on the ice sheet surface and those collected at the margin may be the result of the Yellow Snow and Supraglacial Inland samples having a greater representation in the condensed hydrocarbon region and a lower proportion in the lignin region (Table 4). The grouping of the Subglacial May and Supraglacial Margin samples may be due to greater proportions of protein-like and lipid-like material in these samples compared to the remainder of the dataset (Table 4). The grouping of the Tarn and Subglacial July samples results from a commonality in every region of the van Krevelen plot, particularly in the terrestrial Suwannee River and lignin regions (Table 4).

Apart from these general trends, each sample also has some noteworthy features on the van Krevelen diagram. In addition to a large protein-like component, the Supraglacial Margin sample also contains more formulae in the lipid and the condensed hydrocarbon regions than the Subglacial May sample (Table 4). Even though both the Supraglacial Margin and Subglacial May samples contain lignin-like molecules, the Subglacial May sample has a larger proportion of formulae in the "terrestrial" Suwannee

Please cite this article in press as: Bhatia M. P., et al. Molecular characterization of dissolved organic matter associated with the Greenland ice sheet. *Geochim. Cosmochim. Acta* (2010), doi:10.1016/j.gca.2010.03.035

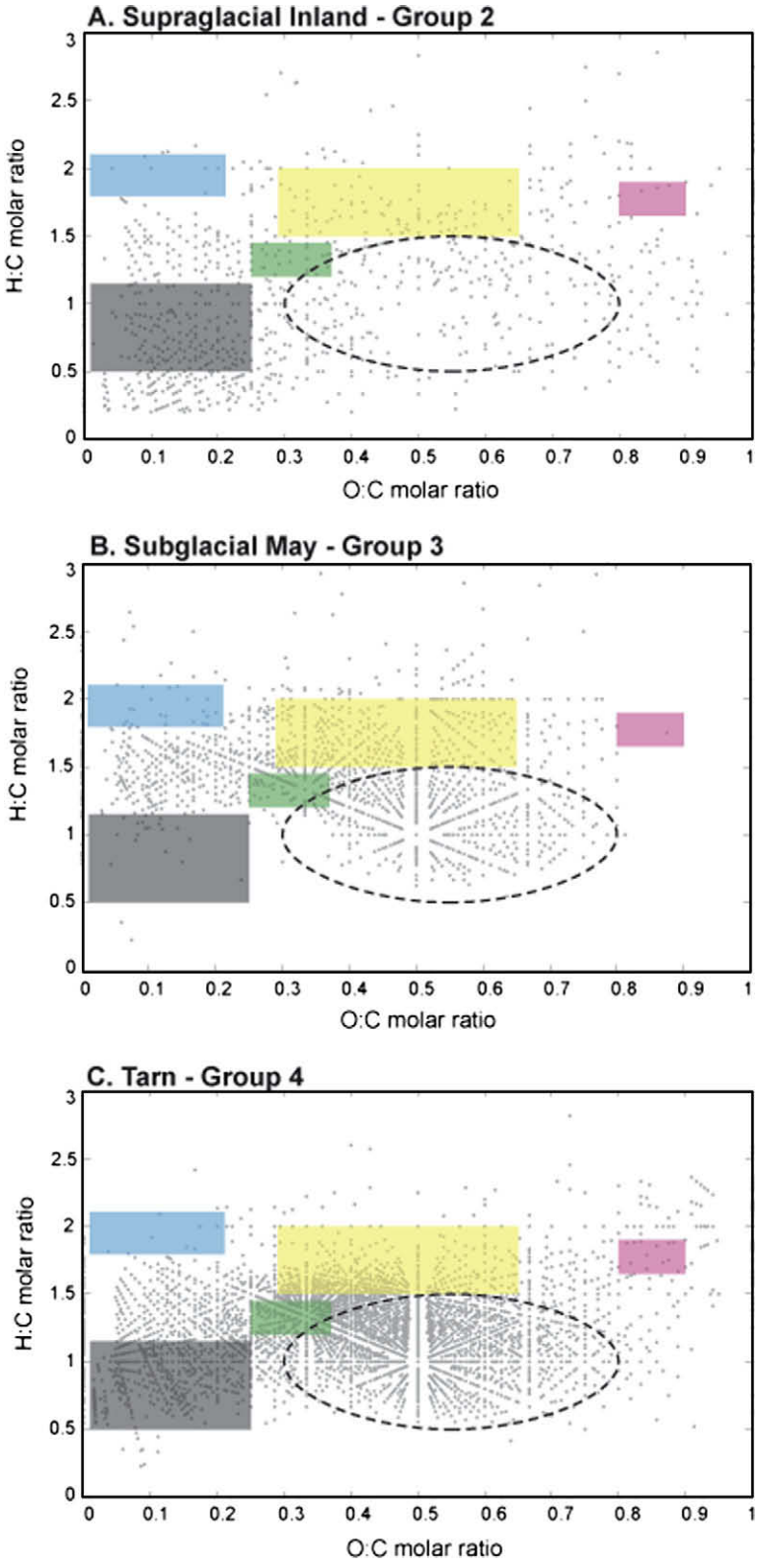

Fig. 4. Van Krevelen diagrams of all formulae assigned (grey dots) to negative ion mode peaks detected within the Supraglacial Inland (A), Subglacial May (B), and Tarn (C) samples. The colored boxes represent elemental compositions for some major compound classes, as approximated from Kim et al. (2003) and Hedges (1990). The grey box represents condensed hydrocarbons, the blue box represents lipids, the green box represents lignin, the yellow box represents proteins, and the pink box represents carbohydrates. The black oval represents elemental formula assignments made for a sample of Suwannee River Fulvic Acid. (For interpretation of the references to colour in this figure legend, the reader is referred to the web version of this article.)

Please cite this article in press as: Bhatia M. P., et al. Molecular characterization of dissolved organic matter associated with the Greenland ice sheet. *Geochim. Cosmochim. Acta* (2010), doi:10.1016/j.gca.2010.03.035

Table 4
Percentage of negative ion mode formula assignments located in different regions of the van Krevelen diagram. Group numbers refer to groups determined by indicator species analysis (see text for details).

Sample	Condensed hydrocarbons	Lipids	Lignin	Protein	Carbohydrate	Terrestrial
Yellow Snow (Group 1)	12.6	1.1	3.0	12.7	0.6	29.2
Supraglacial Inland (Group 2)	16.0	0.5	2.4	9.2	0.6	23.5
Supraglacial Margin (Group 3)	6.8	4.7	3.6	27.0	0.3	14.3
Subglacial May (Group 3)	1.1	1.5	5.5	25.5	0.1	39.2
Subglacial July-1 (Group 4)	6.9	0.9	10.2	10.4	0.1	55.6
Subglacial July-2 (Group 4)	7.8	1.1	8.5	8.4	0.0	55.8
Tarn (Group 4)	9.8	0.1	7.5	13.3	0.3	59.3
Suwannee River	2.0	0.0	4.5	1.9	0.0	85.6

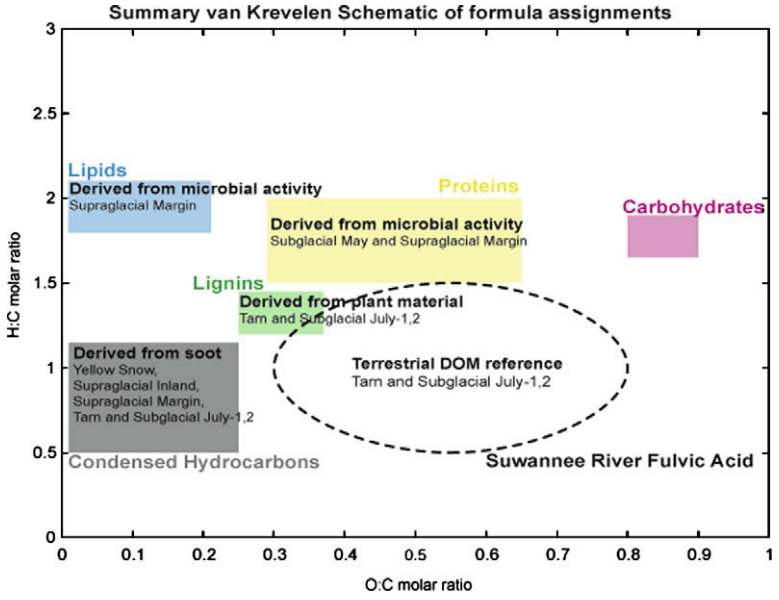

Fig. 5. Van Krevelen diagram summarizing the formula assignments for the negative ion mode samples. The samples/groups containing a high proportion of peaks in the different compound classes are named.

River region (Table 4). The Tarn and Subglacial July samples all contain a larger proportion of formulae in the condensed hydrocarbon and protein regions than the Suwannee River sample (Table 4). The results of our analyses of the van Krevelen plots for each of the samples are summarized in Fig. 5.

Indicator species analysis revealed that a higher content of biologically-derived elemental formulae is responsible for the differentiation of the Subglacial May and Supraglacial Margin samples (Group 3) from the Tarn and Subglacial July samples (Group 4). Indicator *m/z* values for the Group 3 samples are dominated by high H:C compounds occupying the protein region of the van Krevelen diagram (Fig. 6A). Conversely, the indicator *m/z* values for the Group 4 samples are dominated by low H:C compounds found in the terrestrial Suwannee River region. There is a significant terrestrial component within all the ice margin samples, as evidenced by the presence of indicator *m/z* values common to Groups 3 and 4 (yellow dots, Fig. 6B) in this region. This component is absent in the samples collected on the inland ice sheet surface (Yellow Snow and Supraglacial Inland, Groups 1 and 2).

3.4. Potential sources of observed peaks

3.4.1. Microbially-derived material (lipid-like and protein-like signatures)

Similar to previous fluorescence studies (Lafreniere and Sharp, 2004; Barker et al., 2006), the distinct microbial character of the Supraglacial Margin sample (reflected by its high proportion of protein-like formulae) is likely derived from photosynthetic algae and bacteria communities widely observed to be present in supraglacial environments (Carpenter et al., 2000; Grannas et al., 2004; Foreman et al., 2007). The presence of lipid-like material in the Supraglacial Margin sample also correlates well with previous work identifying biologically-derived lipids in organic matter from snow collected at Summit atop the Greenland ice sheet (Grannas et al., 2004; Grannas et al., 2006).

Early season (spring) subglacial waters have also been observed to have a microbial fluorescence signature (Lafreniere and Sharp, 2004; Barker et al., 2006), despite the fact that terrestrial carbon from overridden soils and vegetation is also present at the glacier base (Sharp et al., 1999). The larger proportion of protein-like formulae in

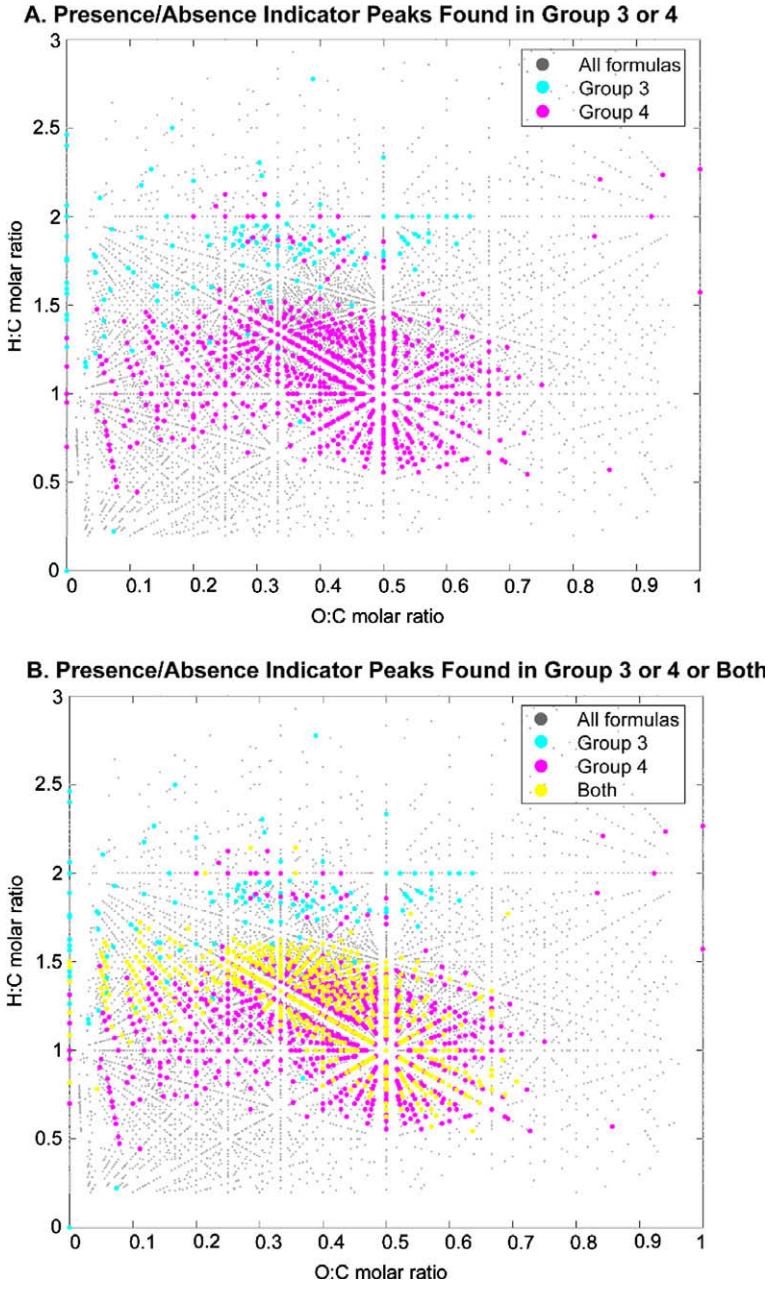

Fig. 6. Van Krevelen negative ion mode diagrams with indicator peaks determined by Indicator Species Analysis. In (A), indicator peaks exclusive to either Group 3 (N glacier May (Subglacial May and Supraglacial Margin)) or Group 4 (terrestrial/N glacier July (Tarn and Subglacial July-1, 2)) are shown; in (B), peaks from (A) are shown as well as indicator peaks found in both Groups 3 and 4.

the early season subglacial waters (Subglacial May) may reflect *in situ* subglacial microbial metabolism of some component of the subglacial organic carbon stores during over winter storage (Tranter et al., 2005). The May subglacial water likely drains a broad distributed hydrological network along the ice–bed interface, and consequently experiences prolonged storage at the bed where active subglacial microbial communities are thought to be present (Tranter et al., 2005). Although no study has documented the presence of subglacial communities beneath the Greenland ice sheet specifically, a mounting body of literature indicates that large, active microbial communities are present beneath glaciers in diverse regions on varying lithologies (the Swiss Alps, southern New Zealand Alps, Alaska, Svalbard, Antarctica, and the Canadian high Arctic) (Sharp et al., 1999; Skidmore et al., 2000; Lanoil et al., 2009; Mikucki et al., 2009). Furthermore, studies show that the abundances of subglacial communities (as high as 1.8×10^9 cells g^{-1}) are similar to the highest microbial abundances in permafrost (10^7–10^9 cells g^{-1}) (Sharp et al., 1999). Documented subglacial communities include heterotrophic bacteria (e.g., aerobic respires, nitrate- and sulfate-

reducers) as well as autotrophic bacteria (e.g., methanogens) (Skidmore et al., 2000; Foght et al., 2004; Cheng and Foght, 2007). The existence of numerically-abundant, enduring biological communities implies that any microbially-mediated biogeochemical activities occur on a continuous temporal basis. The diverse DOM composition in the Subglacial May sample is consistent with the idea of high subglacial microbial activity due in particular to its significant protein and terrestrial components (Table 4).

3.4.2. Terrestrial-derived material (lignins and Suwannee River-like components)

Lignins and formulae located in the "terrestrial" region of our van Krevelen plots are likely derived from previously overridden soils and vegetation (subglacial samples) or surrounding terrestrial soils and vegetation (Tarn). The large component of terrestrially-derived DOM in the Tarn sample (overlap between Suwannee River and the Tarn sample is 70%), is likely derived from its location in the developed soils and vegetation at our study site. In contrast, the subglacial samples contain terrestrially-derived DOM, present in both May and July, that is most likely derived from previously overridden soils and vegetation during glacial advance. The lack of lignin material in the samples collected on the inland ice sheet surface (Yellow Snow, Supraglacial Inland) suggests that organic matter from these environments is not influenced significantly by non-charred terrestrial inputs. This is in contrast to Grannas et al. (2004) who noted the presence of vascular plant tissue (i.e., lignin) in snow collected from Summit, Greenland.

3.4.3. Condensed hydrocarbons

Condensed hydrocarbons are generally compounds with a deficiency in both oxygen and hydrogen and often contain aromatic ring structures. Previous studies have illustrated that these compounds originate from black carbon-like molecules (Kim et al., 2004), and could be derived from atmospheric deposition of soot particles (Slater et al., 2002). Evidence of these compound types is present in all ice sheet surface samples (Yellow Snow, Supraglacial Inland, Supraglacial Margin) and the late/summer discharge samples (Subglacial July-1, 2). On the ice sheet surface, this material likely originates from atmospheric deposition of combustion products. We do not anticipate a novel source of condensed hydrocarbons in the subglacial environment. Rather, the presence of condensed hydrocarbons in late season subglacial waters (Subglacial July-1, 2) may reflect either (1) the increased contribution of supraglacial meltwater to the subglacial outflow at the peak of the summer melt season, or (2) an increased flux of condensed hydrocarbons from the ice sheet surface after the snow cover has melted. Support for this second hypothesis may be provided by Clarke and Noone (1985), who found that soot may be enriched in Arctic snowmelt compared to the snowpack.

3.5. Implications for understanding subglacial flow regimes

The fact that the late season subglacial waters still possess an overwhelming terrestrial signature may reflect the ability of the summer hydrological flow regime to mobilize subglacial organic carbon stores. As the melt season progresses on the Greenland ice sheet, meltwater from seasonal snow and ice collects in streams and lakes on the ice sheet surface. The majority of this surface meltwater is thought to descend to the bed via crevasses and moulins at the peak of the summer melt season (Das et al., 2008; Krawczynski et al., 2009). Thus, the late season subglacial waters are primarily comprised of supraglacial inflow passing rapidly through the subglacial environment. Over the course of a melt season, the ice sheet subglacial drainage system is predicted to evolve from a distributed to a more channelized network facilitating rapid water flow to the glacier front, similar to what has been observed in alpine glacier systems (Nienow et al., 1998). The faster flow rates characteristic of this channelized system do not permit extensive water–sediment interaction, thus minimizing the impact of *in situ* microbial metabolism (Tranter et al., 2005). Additionally, the larger volumes of water passing through the subglacial system may facilitate turbulent incidental contact that allows the meltwaters to mobilize terrestrial sources of DOC at the glacier base (i.e., previously overridden soil and vegetation). Previous work in alpine catchments has illustrated that suspended sediment concentrations increase throughout a melt season as sediment sources are accessed by an extending and integrating subglacial drainage network (Clifford et al., 1995; Richards et al., 1996). This reasoning is also consistent with previous fluorescence spectroscopy work by Barker et al. (2006) at a polythermal Canadian high Arctic glacier, which showed that the late season subglacial meltwaters bear a terrestrially-derived signature. The change in subglacial flow rate may explain why condensed hydrocarbons are not present in the early season subglacial waters. Increased residence times of these waters at the glacier bed throughout the preceding winter would permit non-polar hydrocarbon-like, soot-derived compounds to adsorb quantitatively to organic particles in the subglacial environment (Kramer et al., 2004) and thus to be removed from discharge waters. At the peak of the summer melt season, the higher meltwater flow rates and potentially elevated hydrocarbon concentrations would preclude quantitative removal by adsorption, allowing the subglacial waters to retain these compounds in the late season subglacial runoff.

3.6. Implications for understanding glacial organic matter cycling

The microbial signatures of the subglacial discharge samples analyzed in our study support the suggestion that glacial systems supply labile material to downstream marine and terrestrial environments (Lafreniere and Sharp, 2004; Barker et al., 2006; Hood et al., 2009) extending these results to an ice sheet environment for the first time. This hypothesis follows earlier discoveries of abundant, active microbial communities associated with supraglacial, subglacial, and proglacial environments (Sharp et al., 1999; Anesio et al., 2009; Bhatia et al., 2006). It has been substantiated by direct investigations of glacially-derived DOM, including fluorescence spectrometry (Lafreniere and Sharp, 2004; Barker et al., 2006), compound specific analyses (i.e.

Please cite this article in press as: Bhatia M. P., et al. Molecular characterization of dissolved organic matter associated with the Greenland ice sheet. *Geochim. Cosmochim. Acta* (2010), doi:10.1016/j.gca.2010.03.035

lignin phenols) (Hood et al., 2009), and bulk organic carbon characterizations (C:N ratios, $\delta^{13}C$ values) (Hood and Scott, 2008; Hood et al., 2009). Most recently, Hood et al. (2009) demonstrated that the bioavailability of glacial organic carbon is indirectly correlated with age, so that DOM from glaciated catchments is labile despite having ancient $\Delta^{14}C$ ages. Thus, meltwater streams and rivers draining glaciated areas may potentially provide a significant, previously overlooked source of labile reduced carbon to downstream ecosystems (Barker et al., 2006; Hood et al., 2009). Our study corroborates these findings through a comprehensive molecular-level description of glacially-derived DOM in meltwater runoff from the Greenland ice sheet and offers a novel line of evidence that glacial DOM has a microbial source.

4. CONCLUSIONS

Previous studies illustrate that the majority of supraglacial DOM likely originates from autochthonous microbial processes, whereas subglacial DOM contains both allochthonous carbon derived from previously overridden soils and vegetation, and autochthonous carbon derived from *in situ* microbial metabolism. Our findings support these provenances. Generally the supraglacial and early season subglacial discharge had a higher proportion of protein-like and lipid-like elemental formulae, whereas the tarn and late season subglacial water DOM had a higher proportion of lignin and terrestrial Suwannee River-like materials. However, evolving subglacial flow regimes also likely exert a heavy influence on the type of DOM present in the subglacial outflow at different times of the year. In this study, this influence is reflected in a smaller terrestrial component in the early season subglacial waters, and the detection of condensed hydrocarbon-like material in late season subglacial waters. Based on the samples analyzed, the DOM composition of subglacial outflow shifts from a terrestrial to microbial signature over winter storage and then back to a terrestrial signature through a melt season. We propose that this shift is dependent on the degree of subglacial microbial metabolism that has occurred. However, additional samples and measurements constraining the subglacial flow regime and resident microbial communities are required to fully test the validity of this conjecture.

This study represents the first molecular-level analyses of subglacial organic carbon stores, and as such, has illustrated that ultra-high resolution mass spectrometry can provide unprecedented compositional information regarding the interplay among different glacial carbon pools. In addition to these qualitative results, further work with both bulk and compound-specific measurements will be required to confirm that specific compound classes (e.g., proteins, lipids) are present and to constrain the temporal provenances of these pools. Nevertheless, our results suggest that a much more complex and reactive carbon system is associated with glacial environments than previously thought and merit further investigation, given the extent and frequency of glaciation events through Earth's history.

ACKNOWLEDGEMENTS

This research was supported by: the National Science Foundation (CAREER-OCE-0529101 (E.B.K.), ARC-0520077 (S.B.D.)), National Atmospheric and Space Administration (S.B.D.), the WHOI Clark Arctic Research Initiative (E.B.K., S.B.D., M.-A.C.), the WHOI Ocean Ventures Fund (M.P.B.), and the National and Science Engineering Research Council of Canada (M.P.B.). We acknowledge M. Kido Soule for assistance with data collection and the funding sources of the WHOI FT-MS Users' facility (National Science Foundation OCE-0619608 and the Gordon and Betty Moore Foundation). We are grateful to I. Joughin, M. Behn, R. Harris, B. Gready, P. Henderson, A. Criscitiello, and M. Evans for their assistance in the field, to P. Henderson for conducting the carbon/nitrogen analyses, and to G. Wolken for his assistance in constructing maps of our field site. We also thank three anonymous reviewers whose comments improved the manuscript.

APPENDIX A. SUPPLEMENTARY DATA

Supplementary data associated with this article can be found, in the online version, at doi:10.1016/j.gca.2010.03.035.

REFERENCES

Anesio A. M., Hodson A. J., Fritz A., Psenner R. and Sattler B. (2009) High microbial activity on glaciers: importance to the global carbon cycle. *Global Change Biol.* **15**, 955–960.

Azam F. (1998) Microbial control of oceanic carbon flux: the plot thickens. *Science* **280**, 694–696.

Bamber J. L., Layberry R. L. and Gogineni S. (2001) A new ice thickness and bed data set for the Greenland ice sheet 1. Measurement, data reduction, and errors. *J. Geophys. Res. D: Atmos.* **106**, 33773–33780.

Barker J. D., Sharp M. J., Fitzsimons S. J. and Turner R. J. (2006) Abundance and dynamics of dissolved organic carbon in glacier systems. *Arct. Antarct. Alp. Res.* **38**, 163–172.

Berner R. A., Lasaga A. C. and Garrels R. M. (1983) The carbonate-silicate geochemical cycle and its effect on atmospheric carbon-dioxide over the past 100 million years. *Am. J. Sci.* **283**, 641–683.

Bhatia M., Sharp M. and Foght J. (2006) Distinct bacterial communities exist beneath a high arctic polythermal glacier. *Appl. Environ. Microbiol.* **72**, 5838–5845.

Bingham R. G., Nienow P. W., Sharp M. J. and Boon S. (2005) Subglacial drainage processes at a high Arctic polythermal valley glacier. *J. Glaciol.* **51**, 15–24.

Brown G. H. (2002) Glacier meltwater hydrochemistry. *Appl. Geochem.* **17**, 855–883.

Carpenter E., Lin S. and Capone D. (2000) Bacterial activity in South Pole snow. *Appl. Environ. Microbiol.* **66**, 4514–4517.

Cheng S. M. and Foght J. M. (2007) Cultivation-independent and -dependent characterization of bacteria resident beneath John Evans Glacier. *FEMS Microbiol. Ecol.* **59**, 318–330.

Chillrud S. N., Pedrozo F. L., Temporetti P. F., Planas H. F. and Froelich P. N. (1994) Chemical weathering of phosphate and germanium in glacial meltwaters: effects of subglacial pyrite oxidation. *Limnol. Oceanogr.* **39**, 1130–1140.

Clarke A. D. and Noone K. J. (1985) Soot in the Arctic snowpack: a cause for perturbations in radiative transfer. *Atmos. Environ.* **19**, 2045–2053.

Clifford N. J., Richards K. S., Brown R. A. and Lane S. N. (1995) Scales of variation of suspended sediment concentration and turbidity in a glacial meltwater stream. *Geogr. Ann. Ser. A – Phys. Geogr.* **77A**, 45–65.

Das S. B., Joughin I., Behn M. D., Howat I. M., King M. A., Lizarralde D. and Bhatia M. P. (2008) Fracture propagation to the base of the Greenland Ice Sheet during supraglacial lake drainage. *Science* **320**, 778–781.

Dittmar T., Koch B., Hertkorn N. and Kattner G. (2008) A simple and efficient method for the solid-phase extraction of dissolved organic matter (SPE-DOM) from seawater. *Limnol. Oceanogr. Methods* **6**, 230–235.

Eglinton T. I. and Repeta D. J. (2003) Organic matter in the contemporary ocean. In *Treatise on Geochemistry: Marine Organic Geochemistry*, vol. 6 (ed. H. Elderfield). Elsevier, pp. 145–180.

Foght J., Aislabie J., Turner S., Brown C. E., Ryburn J., Saul D. J. and Lawson W. (2004) Culturable bacteria in subglacial sediments and ice from two Southern Hemisphere glaciers. *Microbiol. Ecol.* **47**, 329–340.

Foreman C. M., Sattler B., Mikucki J. A., Porazinska D. L. and Priscu J. C. (2007) Metabolic activity and diversity of cryoconites in the Taylor Valley, Antarctica. *J. Geophys. Res. Biogeosci.* **112**, 11.

Grannas A. M., Hockaday W. C., Hatcher P. G., Thompson L. G. and Mosley-Thompson E. (2006) New revelations on the nature of organic matter in ice cores. *J. Geophys. Res. D: Atmos.* **111**, D04304.

Grannas A. M., Shepson P. B. and Filley T. R. (2004) Photochemistry and nature of organic matter in Arctic and Antarctic snow. *Global Biogeochem. Cycles* **18**, GB1006.

Hedges J. I. (1990) Compositional indicators of organic acid sources and reactions in natural environments. In *Organic Acids in Aquatic Ecosystems* (eds. E. M. Perdue and E. T. Gjessing). John Wiley & Sons, Ltd..

Hedges J. I., Eglinton G., Hatcher P. G., Kirchman D. L., Arnosti C., Derenne S., Evershed R. P., Kogel-Knabner I., de Leeuw J. W., Littke R., Michaelis W. and Rullkotter J. (2000) The molecularly-uncharacterized component of nonliving organic matter in natural environments. *Org. Geochem.* **31**, 945–958.

Hood E., Fellman J., Spencer R. G. M., Hernes P. J., Edwards R., D'Amore D. and Scott D. (2009) Glaciers as a source of ancient and labile organic matter to the marine environment. *Nature* **462**, 1044–1047.

Hood E. and Scott D. (2008) Riverine organic matter and nutrients in southeast Alaska affected by glacial coverage. *Nat. Geosci.* **1**, 583–587.

Kim S., Kaplan L. A., Benner R. and Hatcher P. G. (2004) Hydrogen-deficient molecules in natural riverine water samples – evidence for the existence of black carbon in DOM. *Mar. Chem.* **92**, 225–234.

Kim S., Kramer R. W. and Hatcher P. G. (2003a) Graphical method for analysis of ultrahigh-resolution broadband mass spectra of natural organic matter, the Van Krevelen diagram. *Anal. Chem.* **75**, 5336–5344.

Kim S., Rodgers R. P. and Marshall A. G. (2006) Truly "exact" mass: elemental composition can be determined uniquely from molecular mass measurement at similar to 0.1 mDa accuracy for molecules up to similar to 500 Da. *Int. J. Mass Spectrom.* **251**, 260–265.

Kim S., Simpson A. J., Kujawinski E. B., Freitas M. A. and Hatcher P. G. (2003b) High resolution electrospray ionization mass spectrometry and 2D solution NMR for the analysis of DOM extracted by C-18 solid phase disk. *Org. Geochem.* **34**, 1325–1335.

Koch B. P., Ludwichowski K. U., Kattner G., Dittmar T. and Witt M. (2008) Advanced characterization of marine dissolved organic matter by combining reversed-phase liquid chromatography and FT-ICR-MS. *Mar. Chem.* **111**, 233–241.

Koch B. P., Witt M. R., Engbrodt R., Dittmar T. and Kattner G. (2005) Molecular formulae of marine and terrigenous dissolved organic matter detected by electrospray ionization Fourier transform ion cyclotron resonance mass spectrometry. *Geochim. Cosmochim. Acta* **69**, 3299–3308.

Kramer R. W., Kujawinski E. B. and Hatcher P. G. (2004) Identification of black carbon derived structures in a volcanic ash soil humic acid by Fourier transform ion cyclotron resonance mass spectrometry. *Environ. Sci. Technol.* **38**, 3387–3395.

Krawczynski M. J., Behn M. D., Das S. B. and Joughin I. (2009) Constraints on the lake volume required for hydro-fracture through ice sheets. *Geophys. Res. Lett.* **36**, L10501.

Kujawinski E. B. (2002) Electrospray ionization Fourier transform ion cyclotron resonance mass spectrometry (ESI FT-ICR MS): characterization of complex environmental mixtures. *Environ. Forensics* **3**, 207–216.

Kujawinski E. B. and Behn M. D. (2006) Automated analysis of electrospray ionization Fourier transform ion cyclotron resonance mass spectra of natural organic matter. *Anal. Chem.* **78**, 4363–4373.

Kujawinski E. B., Longnecker K., Blough N. V., Vecchio R. D., Finlay L., Kitner J. B. and Giovannoni S. J. (2009) Identification of possible source markers in marine dissolved organic matter using ultrahigh resolution mass spectrometry. *Geochim. Cosmochim. Acta* **73**, 4384–4399.

Lafreniere M. J. and Sharp M. J. (2004) The concentration and fluorescence of dissolved organic carbon (DOC) in glacial and nonglacial catchments: interpreting hydrological flow routing and DOC sources. *Arct. Antarct. Alp. Res.* **36**, 156–165.

Lanoil B., Skidmore M., Priscu J. C., Han S., Foo W., Vogel S. W., Tulaczyk S. and Engelhardt H. (2009) Bacteria beneath the West Antarctic Ice Sheet. *Environ. Microbiol.* **11**, 609–615.

Layberry R. L. and Bamber J. L. (2001) A new ice thickness and bed data set for the Greenland ice sheet 2. Relationship between dynamics and basal topography. *J. Geophys. Res. D: Atmos.* **106**, 33781–33788.

Lyons W. B., Welch K. A. and Doggett J. K. (2007) Organic carbon in Antarctic snow. *Geophys. Res. Lett.* **34**.

Mantini D., Petrucci F., Pieragostino D., Del Boccio P., Di Nicola M., Di Ilio C., Federici G., Sacchetta P., Comani S. and Urbani A. (2007) LIMPIC: a computational method for the separation of protein MALDI-TOF-MS signals from noise. *BMC Bioinf.* **8**.

Marshall A. G. and Rodgers R. P. (2008) Petroleomics: chemistry of the underworld. *Proc. Nat. Acad. Sci. USA* **105**, 18090–18095.

McCune B. and Grace J. 2002. *Analysis of Ecological Communities*. MjM Software Design, Gleneden Beach, Oregon.

McKnight D. M., Andrews E. D., Spaulding S. A. and Aiken G. R. (1994) Aquatic fulvic acids in algal rich antarctic ponds. *Limnol. Oceanogr.* **39**, 1972–1979.

McKnight D. M., Boyer E. W., Westerhoff P. K., Doran P. T., Kulbe T. and Andersen D. T. (2001) Spectrofluorometric characterization of dissolved organic matter for indication of precursor organic material and aromaticity. *Limnol. Oceanogr.* **46**, 38–48.

Mikucki J. A., Pearson A., Johnston D. T., Turchyn A. V., Farquhar J., Schrag D. P., Anbar A. D., Priscu J. C. and Lee P. A. (2009) A contemporary microbially maintained subglacial ferrous "ocean". *Science* **324**, 397–400.

Please cite this article in press as: Bhatia M. P., et al. Molecular characterization of dissolved organic matter associated with the Greenland ice sheet. *Geochim. Cosmochim. Acta* (2010), doi:10.1016/j.gca.2010.03.035

Nienow P., Sharp M. and Willis I. C. (1998) Seasonal changes in the morphology of the subglacial drainage system, Haut Glacier d'Arolla, Switzerland. *Earth Surf. Process. Landf.* **23**, 825–843.

Raiswell R. (1984) Chemical models of solute acquisition in glacial meltwaters. *J. Glaciol.* **30**, 49–57.

Reemtsma T., These A., Linscheid M., Leenheer J. and Spitzy A. (2008) Molecular and structural characterization of dissolved organic matter from the deep ocean by FTICR-MS, including hydrophilic nitrogenous organic molecules. *Environ. Sci. Technol.* **42**, 1430–1437.

Richards K., Sharp M., Arnold N., Gurnell A., Clark M., Tranter M., Nienow P., Brown G., Willis I. and Lawson W. (1996) An integrated approach to modelling hydrology and water quality in glacierized catchments. *Hydrol. Processes* **10**, 479–508.

Sharp M., Parkes J., Cragg B., Fairchild I. J., Lamb H. and Tranter M. (1999) Widespread bacterial populations at glacier beds and their relationship to rock weathering and carbon cycling. *Geology* **27**, 107–110.

Skidmore M., Anderson S. P., Sharp M., Foght J. and Lanoil B. D. (2005) Comparison of microbial community compositions of two subglacial environments reveals a possible role for microbes in chemical weathering processes. *Appl. Environ. Microbiol.* **71**, 6986–6997.

Skidmore M. L., Foght J. M. and Sharp M. J. (2000) Microbial life beneath a high Arctic glacier. *Appl. Environ. Microbiol.* **66**, 3214–3220.

Slater J. F., Currie L. A., Dibb J. E. and Benner B. A. (2002) Distinguishing the relative contribution of fossil fuel and biomass combustion aerosols deposited at Summit, Greenland through isotopic and molecular characterization of insoluble carbon. *Atmos. Environ.* **36**, 4463–4477.

Sleighter R. L. and Hatcher P. G. (2008) Molecular characterization of dissolved organic matter (DOM) along a river to ocean transect of the lower Chesapeake Bay by ultrahigh resolution electrospray ionization Fourier transform ion cyclotron resonance mass spectrometry. *Mar. Chem.* **110**, 140–152.

Southam A. D., Payne T. G., Cooper H. J., Arvanitis T. N. and Viant M. R. (2007) Dynamic range and mass accuracy of wide-scan direct infusion nanoelectrospray Fourier transform ion cyclotron resonance mass spectrometry-based metabolomics increased by the spectral stitching method. *Anal. Chem.* **79**, 4595–4602.

Stenson A. C., Marshall A. G. and Cooper W. T. (2003) Exact masses and chemical formulas of individual Suwannee River fulvic acids from ultrahigh resolution electrospray ionization Fourier transform ion cyclotron resonance mass spectra. *Anal. Chem.* **75**, 1275–1284.

Tranter M., Sharp M. J., Lamb H. R., Brown G. H., Hubbard B. P. and Willis I. C. (2002) Geochemical weathering at the bed of Haut Glacier d'Arolla, Switzerland – a new model. *Hydrol. Processes* **16**, 959–993.

Tranter M., Skidmore M. and Wadham J. (2005) Hydrological controls on microbial communities in subglacial environments. *Hydrol. Processes* **19**, 995–998.

Wadham J. L., Tranter M., Tulaczyk S. and Sharp M. (2008) Subglacial methanogenesis: a potential climatic amplifier? *Global Biogeochem. Cycles* **22**, GB2021.

Wu Z., Rodgers R. P. and Marshall A. G. (2004) Two- and three-dimensional van krevelen diagrams: a graphical analysis complementary to the kendrick mass plot for sorting elemental compositions of complex organic mixtures based on ultrahigh-resolution broadband fourier transform ion cyclotron resonance mass measurements. *Anal. Chem.* **76**, 2511–2516.

Associate editor: Carol Arnosti